ELSEVIER

Ceramics International 33 (2007) 987–991

CERAMICS INTERNATIONAL

www.elsevier.com/locate/ceramint

Reactions in hydroxylapatite–zirconia composites

Zafer Evis *

Middle East Technical University, Department of Engineering Sciences, 06531 Ankara, Turkey

Received 15 September 2005; received in revised form 23 December 2005; accepted 22 February 2006
Available online 18 April 2006

Abstract

Sintered composites of hydroxylapatite (HA) and zirconia were studied with X-ray diffraction and scanning electron microscopy (SEM). Addition of zirconia caused increased decomposition of the HA in composites sintered at 1100 °C and 1300 °C, forming tricalcium phosphate phases (TCP). The volume of the unit cell of HA increased as the concentration of zirconia in the composites increased. These results are explained as resulting from exchange of Ca^{2+} and ZrO^{2+} ions between the HA and the zirconia. The porosity of the sintered composites increased with increase in zirconia concentration in the composites, probably because of water formed by the decomposition of the HA.

Keywords: A. Sintering; B. X-ray methods; D. Apatite; D. ZrO_2

1. Introduction

Hydroxylapatite (HA, $Ca_{10}(PO_4)_6(OH)_2$) has been widely used as a bulk implant in non-load bearing areas of the body and as coatings on implant metals [1,2]. HA is mainly used as a hard tissue implant because of its excellent biocompatibility in the human body. An HA implant can only be used in non-load bearing areas because of its brittle nature. Inert crystalline ceramics (e.g. zirconia) can be mixed with HA to make composites that take advantage of the biocompatibility of HA and high strength of zirconia.

When HA-inert ceramic composites are air sintered from 1100 °C to 1400 °C, HA decomposes to form unwanted second phases (i.e. α-tri calcium phosphate) [1,2]. When H_2O vapor is present during sintering, the removal of OH^- bonds from the HA phase is minimized making it stable to higher temperatures. HA in composites can be made more resistant to high temperature decomposition by substituting small amounts of impurities in the HA phase, such as Na^+, Mg^{2+}, CO_3^{2-}, F^- or by adding a third ceramic material such as CaF_2 [3,4].

Because of its high mechanical strength, toughness, and inertness in the human body, zirconia improves the properties of HA as a second phase. HA–zirconia composites can be produced by two methods. In the first, calcium phosphate and zirconia powders are mixed, cold pressed and then sintered at higher temperatures in different environments [2,5–9]. In the second, HA–zirconia composites are synthesized by precipitation from solutions of $ZrOCl_2{\cdot}8H_2O$, calcium nitrate and ammonium phosphate to form HA and zirconia crystals [10–12].

Although pure HA starts to decompose to TCP second phases at temperatures above 1300 °C, second phase formation starts well below 1300 °C in the presence of ZrO_2 [5,9,13]. Two of these decomposition reactions are [5,13]:

$$Ca_{10}(PO_4)_6(OH)_2 \rightarrow 3Ca_3(PO_4)_2 + CaO + H_2O \quad (1)$$

$$Ca_{10}(PO_4)_6(OH)_2 + ZrO_2 \rightarrow 3Ca_3(PO_4)_2 + CaZrO_3 + H_2O \quad (2)$$

In the presence of zirconia the calcium oxide formed in Eq. (1) can either form $CaZrO_3$ as shown in Eq. (2), or dissolve in the zirconia to form calcium-stabilized zirconia. In the latter case either tetragonal or cubic zirconia is preserved at room temperature, instead of the monoclinic phase that is stable in pure zirconia at room temperature.

Above 1125 °C, β-$Ca_3(PO_4)_2$ transforms to α-$Ca_3(PO_4)_2$, which has lower density (2.86 as compared to 3.07 for β).

The purpose of the present study was to examine processing methods of HA–zirconia composites, and to characterize the resulting composites with X-ray diffraction, density, and electron microscope measurements. Mechanisms of reactions between HA and zirconia were deduced from these experimental results.

* Tel.: +90 312 210 4450; fax: +90 312 210 4462.
E-mail address: evis@metu.edu.tr.

0272-8842/$32.00
doi:10.1016/j.ceramint.2006.02.012

2. Experimental methods

2.1. Synthesis

Pure HA and HA–zirconia composites were synthesized by precipitation methods [14].

For the HA synthesis, 0.5 M $Ca(NO_3)_2{\cdot}4H_2O$ and 0.3 M $(NH_4)_2HPO_4$ were dissolved in distilled water separately. The Ca/P ratio should be 1.67 when these solutions are mixed to produce stoichiometric HA. NH_4OH was added to both of these solutions to bring the pH level to 11–12. Then calcium nitrate solution was added drop wise into the continuously stirred ammonium phosphate solution. The vigorous stirring produced a milky-gelatinous solution. After stirring the HA solution at RT for 2–3 h, it was heated to 90 °C for 1 h during stirring. Then the solution was stirred for 1 day at RT. In the next step, the solution was washed repeatedly to remove the remaining ammonia and then filtered using a fine filter paper. The filtered wet cake was dried in the oven at 60–90 °C overnight to remove the excess water. Finally the dried cake was sintered at 1100 °C or 1300 °C for 1 h; it was heated and cooled in the furnace.

HA–ZrO_2 composites were synthesized by a precipitation method. $ZrOCl_2{\cdot}8H_2O$ was dissolved in distilled water and the pH was brought to 11–12. Then this solution was added drop wise into an ammonium phosphate solution. Finally, calcium nitrate solution was added drop wise into this solution. The Ca/P ratio was kept at 1.67, as in stoichiometric HA synthesis. To produce 3, 5.8 and 8.4 wt.% ZrO_2–HA composites, 0.25, 0.5 and 0.75 mol of $ZrOCl_2{\cdot}8H_2O$ was added into the solution for every 10 mol of $Ca(NO_3)_2{\cdot}4H_2O$. All the other steps were the same as the HA synthesis.

2.2. Characterization methods

X-ray diffraction (XRD) was performed on all the samples to determine the phases present in the composites and the hexagonal lattice parameters (a and c) of HA. A Scintag XRD diffractometer (Sunnyvale, CA) with a Cu Kα radiation at 50 kV and 30 mA was used to scan the diffraction 2θ angles from 20° to 50° with a speed of $1^\circ\,\mathrm{min}^{-1}$. XRD angle positions were used to calculate the hexagonal unit lattice parameters of the pure HA and the HA in the composites by an iteration method. The volume of the each unit cell was calculated by the following formula $V = 2.589a^2c$. To determine the phases present, XRD peak positions were compared with JCPDS files.

The relative amounts of phases were determined from the most intense X-ray diffraction peaks of the phases present (HA, α and β TCP and ZrO_2) [15]. The heights of the zirconia (tetragonal) peaks are roughly proportional to the concentrations of zirconia originally added to the mixture, so it is assumed that the zirconia concentrations are these original amounts.

It is assumed that the concentrations (wt.%) of HA and TCP phases are proportional to their peak heights in the mixtures. First the ratio R_O of the peak heights of HA to that of α or β TCP was determined for mixtures of known concentrations of HA and α or β TCP. It was found that the ratio R_O did not depend on the relative amounts of HA and TCP; the values of R_O found were 1.755 for $R_O = I_H/I_\beta$ and $R_O = I_H/I_\alpha = 2.217$, where I_H, I_β and I_α are the X-ray diffraction peak heights for HA, β TCP and α TCP, respectively, in mixtures of known concentrations. Then for mixtures of HA and β TCP:

$$\frac{W_H}{W_\beta} = \frac{R}{R_O} \tag{3}$$

where W_H and W_β are the weight fractions of HA and β TCP, respectively. A similar formula for mixtures of HA and α TCP, with W_α substituted for W_β, was used.

For mixtures or composites containing three phases, HA, TCP, and ZrO_2:

$$W_H + W_B + W_Z = 1 \tag{4}$$

where W_Z is the weight fraction of zirconia, from the original mixture. Then,

$$W_H = \frac{R/R_O(1 - W_Z)}{1 + (R/R_O)} \tag{5}$$

where R_O is the value given above for either α or β TCP.

Sample surfaces were examined in a JOEL (JSM-840) scanning electron microscope (SEM) at 15 kV to determine the grain size and porosity in the composites. Polished surfaces were etched in 0.15 M lactic acid for 10 s and rinsed in water and dried. Then they were coated with gold in vacuum before examination in the SEM. Grain size was determined by the intercept method [16].

3. Results

Porosities of the composites as determined from SEM are given in Table 1. Addition of ZrO_2 to the mixture gave increased porosity, especially at 1100 °C. There might be substantial sampling errors in determining the porosities from the SEM micrographs (see Figs. 1–3), so the values in Table 1 are only semi-quantitative.

The average grain size determined from the micrographs are given in Table 2. For sintering at 1100 °C the grain size in pure HA was smaller than in the composites containing ZrO_2, but for sintering at 1300 °C, the addition of ZrO_2 at all concentrations substantially decreased the grain size in the composites.

The phases present for different ZrO_2 concentrations and sintering temperatures can be deduced from the X-ray diffraction patterns in Fig. 4. When pure HA was sintered at 1100 °C (pattern A) there was no evidence for decomposition of the HA. When 3, 5.8 and 8.4 wt.% ZrO_2–HA composites were

Table 1
Percent porosity of HA–zirconia composites

Mixture wt.% ZrO_2	1100 °C	1300 °C
HA	0.9 ± 0.2	0.2 ± 0.1
HA + 3% ZrO_2	8.0 ± 1.1	0.6 ± 0.1
HA + 5.8% ZrO_2	4.9 ± 0.9	2.4 ± 0.5
HA + 8.4% ZrO_2	5.8 ± 0.7	0.5 ± 0.2

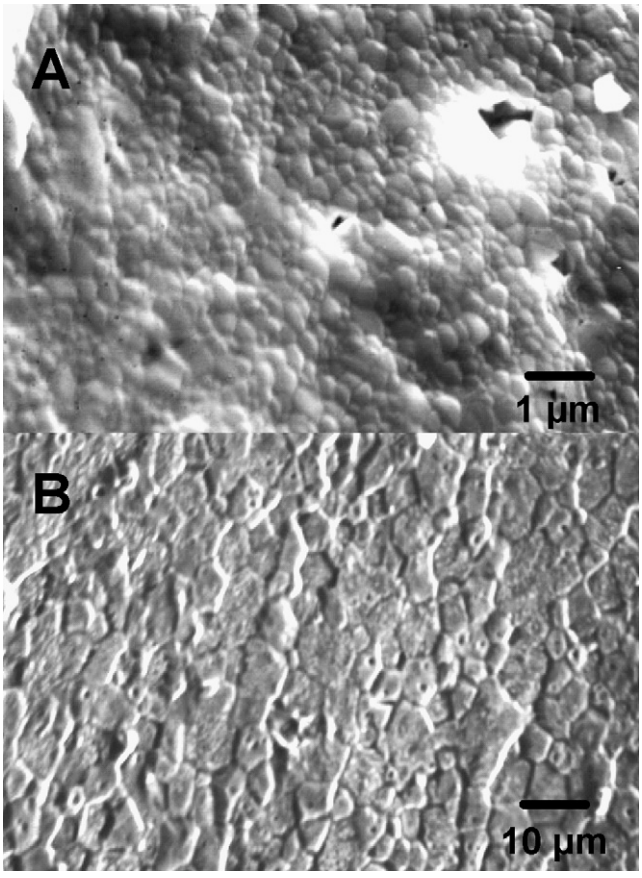

Fig. 1. SEM micrographs of sintered HA. (A) 1100 °C (×10,000), (B) 1300 °C (×1000).

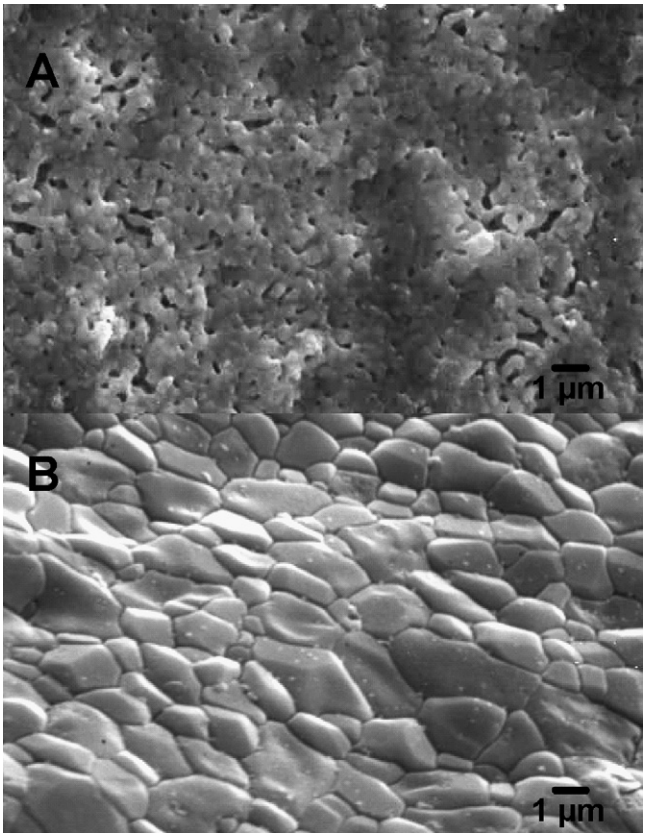

Fig. 2. SEM micrographs of sintered composites of 97% wt.% HA and 3 wt.% ZrO_2. (A) 1100 °C (×5000), (B) 1300 °C (×5000).

sintered at 1100 °C, the HA phase partially transformed to the TCP ($Ca_3(PO_4)_2$) phase, which had the β structure, whereas for sintering at 1300 °C it had α structure.

The amounts of HA in the composites as calculated from the intensities of the X-ray diffraction lines and Eq. (5) are given in Table 3. The decomposition of HA was greater at 1300 °C than at 1100 °C, especially for the higher ZrO_2 concentrations.

The lattice parameters for HA in the composites as calculated from the angles of X-ray diffraction peaks are given in Table 4. The volume of the unit cell in sintered HA increased as the amount of ZrO_2 in the composites increased, especially at 1100 °C. These increases in volume resulted mainly from increases in the *a* parameters, rather than the *c* values.

4. Discussion

The increased tendency of decomposition of HA with reaction with ZrO_2 can be explained as resulting from removal of calcium from the HA and its dissolution into the zirconia. This solid solution of calcium into the zirconia leads to its transformation to the tetragonal phase. It is proposed that the removal of calcium ions from HA involves an ion exchange reaction with ZrO^{2+} ions from the zirconia. Monoxides of four-valent ions, such as CO and SiO, are stable even at room temperature, and are increasingly stable at higher temperatures [18]. The radius of a calcium ion is about 0.1 nm; that of ZrO^{2+} is about 0.21 nm [19]. Thus, when the ZrO^{2+} ion is substituted for Ca^{2+}, the volume of the unit cell of the HA is increased. This exchange therefore explains the increase of volume of the unit cell as shown in Table 4. It is unlikely that the Zr^{4+} ion substitutes for phosphorous in the HA structure, because the Zr^{4+} ion is much larger than the phosphorous ion. The ionic radii are 0.38 nm for P^{5+} and 0.72 nm for Zr^{4+}.

In the zirconia the exchange of Ca^{2+} for a ZrO^{2+} unit leads to a smaller unit cell volume and transformation of the zirconia from monoclinic to tetragonal phase. The tetragonal phase has a higher density (6.10 g/cm^3) than the monoclinic phase (5.68 g/cm^3).

The structure of zirconia in the composites was tetragonal after sintering at both 1100 °C and 1300 °C. The structure of pure zirconia is monoclinic up to about 1180 °C [17], where it transforms to tetragonal structure. There is considerable solid solution of CaO zirconia at high temperatures, and this addition of CaO reduces the stability of m-ZrO_2 so that when more than about 1% CaO dissolves in the zirconia at 1100 °C, the m-ZrO_2 transforms to tetragonal phase [17]. Cubic zirconia is also stable in certain CaO concentrations and temperatures, but the X-ray diffraction lines for tetragonal and cubic zirconia are so similar that it was difficult to distinguish these two phases in our diffraction patterns.

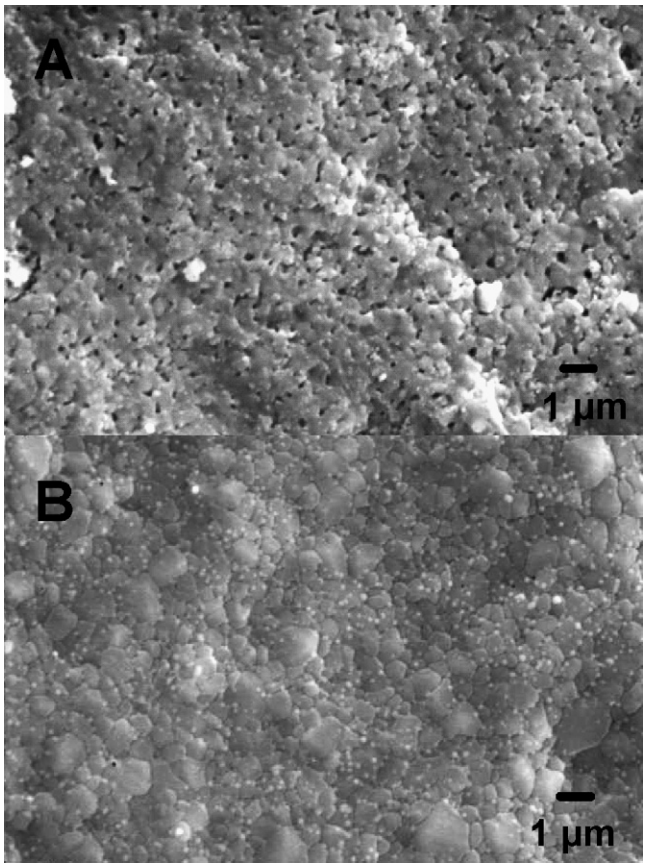

Fig. 3. SEM micrographs of sintered composites of 91.6 wt.% HA and 8.4 wt.% ZrO_2. (A) 1100 °C (×5000), (B) 1300 °C (×5000).

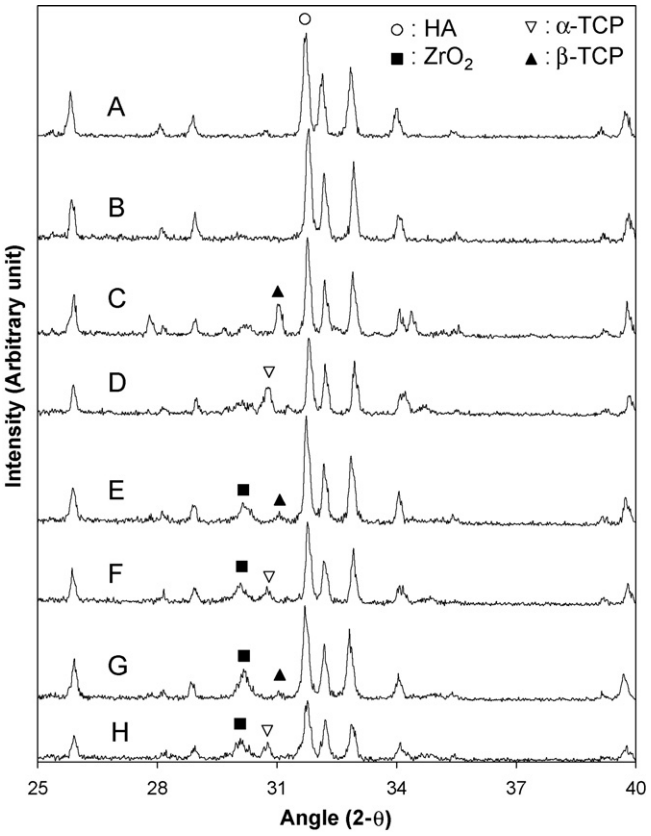

Fig. 4. X-ray diffraction patterns of sintered samples. A and B: HA at 1100 °C and 1300 °C; C and D: 3% ZrO_2 at 1100 °C and 1300 °C; E and F: 5.8% ZrO_2 at 1100 °C and 1300 °C; G and H: 8.4% ZrO_2 at 1100 °C and 1300 °C.

Table 2
Average grain sizes of HA–zirconia composites, as measured from SEM

Mixture wt.% ZrO_2	Average grain size (μm)	
	1100 °C	1300 °C
HA	0.26 ± 0.04	4.44 ± 0.72
HA + 3% ZrO_2	0.54 ± 0.07	1.14 ± 0.21
HA + 5.8% ZrO_2	0.50 ± 0.08	1.11 ± 0.13
HA + 8.4% ZrO_2	0.42 ± 0.05	0.73 ± 0.09

Table 3
Weight fraction W_H of HA in composites after sintering, from the intensities of X-ray lines and Eq. (5)

Mixture wt.% ZrO_2	W_H	
	1100 °C	1300 °C
3	0.63	0.57
5.8	0.81	0.66
8.4	0.80	0.58

The exchange of Ca^{2+} and ZrO^{2+} ions can occur where the surfaces of ZrO_2 and HA are in contact, with minimum rearrangement of their structures. Different apatites can have many substitute ions in their structures without causing change from the HA structure [20].

The exchange of ZrO^{2+} ions for Ca^{2+} ions in the HA structure explains the increased tendency of the exchanged HA to decompose. The large ZrO^{2+} ion introduces strain into the HA network structure, making the decomposition of Eq. (1) more favorable.

Table 4
Lattice parameters *a* and *c* for HA in HA–zirconia composites and volume and volume changes of the unit cell

Mixture	Lattice parameters (Å)				Volume (Å^3)		ΔVol. (Å^3)	
	a, 1100 °C	*c*, 1100 °C	*a*, 1300 °C	*c*, 1300 °C	1100 °C	1300 °C	1100 °C	1300 °C
HA	9.4269 (4)	6.8888 (9)	9.4188 (5)	6.8853 (6)	1582.8	1581.6	0	−1.4
HA + 3 wt.% ZrO_2	9.4350 (6)	6.8834 (5)	9.4223 (7)	6.8877 (1)	1586.4	1582.5	3.6	0.3
HA + 5.8 wt.% ZrO_2	9.4417 (9)	6.8876 (7)	9.4296 (3)	6.8904 (7)	1589.6	1586.2	6.8	3.4
HA + 8.4 wt.% ZrO_2	9.4566 (5)	6.8785 (7)	9.4331 (9)	6.8850 (6)	1592.6	1586.2	9.8	3.4

In HA–ZrO_2 composites containing10 wt.% ZrO_2 or more, $CaZrO_3$ is formed after reaction between 1200 °C and 1300 °C [21]. This result and the present ones suggest that for smaller amounts of ZrO_2 in the composites all the calcium formed by Eq. (1) is dissolved in the ZrO_2, but when the solubility limit of CaO in the ZrO_2 is reached, more calcium reacts with the zirconia to form $CaZrO_3$ by reaction (2).

The increased porosity in the sintered composites with addition of zirconia probably results because of the water generated by decomposition of the HA (reaction (1)). This water is held in pores formed during sintering, and must diffuse out of the HA matrix, in addition to other trapped gases, to form dense HA.

5. Conclusion

High density HA–ZrO_2 composites (more than 92% of the theoretical density) were produced after the synthesis by precipitation method and air sintering at 1100 °C and 1300 °C without any need to pressure sintering. The decomposition of HA during sintering at 1100 °C and 1300 °C is increased by addition of zirconia. This decomposition involves the exchange of Ca^{+2} and ZrO^{2+} ions between the HA and zirconia. The larger ZrO^{2+} ions cause swelling of the HA structure, and the resulting strain increases the rate of decomposition of the HA. Water generated by this decomposition leads to increased porosity of the sintered composites.

References

[1] H. Ji, P.M. Marquis, Sintering behavior of hydroxyapatite reinforced with 20 wt.% Al_2O_3, J. Mater. Sci. 28 (1993) 1941–1945.

[2] T. Matsuno, K. Watanabe, K. Ono, M. Koishi, Preparation of laminated hydroxyapatite/zirconia sintered composite with the gradient composition, J. Mater. Sci. Lett. 17 (1998) 1349–1351.

[3] R. Kijkowska, S. Lin, R.Z. LeGeros, Physico-chemical and thermal properties of chlor-, fluor-, and hydroxyapatites, in: S. Brown, I. Clarke, P. Williams (Eds.), Bioceramics, vol. 14, Trans Tech Publications Ltd, Switzerland, 2002, p. 31.

[4] J.C. Elliot, Structure and Chemistry of the Apatites and other Calcium Orthophosphates, Elsevier, Amsterdam, 1994.

[5] H.W. Kim, Y.J. Noh, Y.H. Koh, H.E. Kim, H.M. Kim, Effect of CaF_2 on densification and properties of hydroxyapatite–zirconia composites for biomedical applications, Biomaterials 23 (2002) 4113–4121.

[6] R.B. Heimann, T.A. Vu, Effect of CaO on thermal decomposition during sintering of composite hydroxyapatite–zirconia mixtures for monolithic bioceramic implants, J. Mater. Sci. Lett. 16 (1997) 437–439.

[7] J. Li, H. Liao, L. Hermansson, Sintering of partially-stabilized zirconia and partially-stabilized zirconia–hydroxyapatite composites by hot isostatic pressing and pressureless sintering, Biomaterials 17 (1996) 1787–1790.

[8] M. Takagi, M. Mochida, N. Uchida, K. Saito, K. Uematsu, Filter cake forming and hot isostatic pressing for TZP-dispersed hydroxyapatite composite, J. Mater. Sci.: Mater. Med. 3 (1992) 199–203.

[9] R.R. Rao, T.S. Kannan, Synthesis and sintering of hydroxyapatite–zirconia composites, Mater. Sci. Eng. C 20 (2002) 187–193.

[10] K. Ioku, M. Yoshimura, S. Somiya, Microstructure and mechanical properties of hydroxyapatite ceramics with zirconia dispersion prepared by post-sintering, Biomaterials 11 (1990) 57–61.

[11] E.S. Ahn, N.J. Gleason, A. Nakahira, J.Y. Ying, Nanostructure processing of hydroxyapatite-based bioceramics, Nano Lett. 1–3 (2001) 149–153.

[12] J. Wu, T. Yeh, Sintering of hydroxyapatite–zirconia composite materials, J. Mater. Sci. 23 (1988) 3771–3777.

[13] E. Chang, W.J. Chang, B.C. Wang, C.Y. Yang, Plasma spraying of zirconia-reinforced hydroxyapatite composite coatings on titanium, J. Mater. Sci.: Mater. Med. 8 (1997) 193–200.

[14] M. Jarcho, C.H. Bolen, M.B. Thomas, J. Babock, J.F. Kay, R.H. Doremus, Hydroxylapatite synthesis and characterization in dense polycrystalline form, J. Mater. Sci. 11 (1976) 2027–2035.

[15] B.D. Cullity, Elements of X-ray Diffraction, second ed., Addison-Wesley, Reading, MA, 1978, Section 14–10.

[16] J.E. Hilliard, Estimating grain size by the intercept method, Metal Progress Data Sheet (1964) 99–102.

[17] A.E. McHale, R.S. Roth, Phase Equilibrium Diagrams, vol. XII, Am. Ceramic Soc., Westerville, OH, 1996, Diagrams 9898 and 9899.

[18] R.H. Doremus, Diffusion of Reactive Molecules in Solids and Melts, Wiley, 2002, p. 70.

[19] J.S.O. Evans, T.A. Mary, T. Vogt, M.A. Subramanian, A.W. Sleight, Negative thermal expansion in ZrW_2O_8 and HfW_2O_8, Chem. Mater. 8 (1996) 2809–2823.

[20] R.V. Gaines, H.C.W. Skinner, E.E. Foord, B. Mason, A. Rosenzweig, Dana's New Minerology, eighth ed., Wiley, 1997, p. 854.

[21] Z. Evis, C. Ergun, R.H. Doremus, Hydroxylapatite–zirconia composites: thermal stability of phases and sinterability as related to the CaO–ZrO_2 phase diagram, J. Mater. Sci. 40 (2005) 1127.